Suite 2101 – 4464 Markham Street
Victoria, British Columbia, V8Z 7X8, Canada

Phone: +1.250.483.3300 Fax: +1.250.483.3301
Email: info@jasco.com Website: www.jasco.com

Sound pressure and particle velocity measurements from marine pile driving at Eagle Harbor maintenance facility, Bainbridge Island WA

by Alex MacGillivray and Roberto Racca

JASCO Research Ltd
Suite 2101-4464 Markham St.
Victoria, British Columbia
V8Z 7X8 Canada

prepared for Washington State Department of Transportation

November 2005

TABLE OF CONTENTS

1. Introduction 1
2. Project description 1
3. Experimental description 2
4. Methodology 4
   4.1. Theory 4
   4.2. Measurement apparatus 5
   4.3. Data processing 6
   4.4. Acoustic metrics 7
      4.4.1. Sound pressure levels 7
      4.4.2. Particle velocity levels 8
5. Measurement results 8
6. Summary 13
7. Literature cited 13

Version	Date	Description	Author
1.0	28 Nov 2005	Initial draft.	Alex MacGillivray
1.1	29 Nov 2005	Editorial Revisions; checked field information.	Roberto Racca
1.2	29 Nov 2005	Changed layout of figures and accepted tracked changes. Added title page and table of contents.	Alex MacGillivray
1.3	02 Jan 2006	Fixed erroneous dates. Changed scales on velocity trace plots. Added construction details for bubble curtain. Addressed Jim Laughlin's comments on the text of the report.	Alex MacGillivray
1.4	23 Jan 2006	Added description of project provided by Ellie Ziegler.	Alex MacGillivray

1. Introduction

On 31 October 2005, JASCO Research Ltd performed measurements of underwater acoustic pressure and particle velocity from marine pile driving at the Washington State Ferries (WSF) Eagle Harbor maintenance facility located on Bainbridge Island in Washington State. Ten piles were being installed at the ferries' maintenance facility as part of a construction project to upgrade a walk-on slip to a drive-on slip. Underwater measurements of acoustic pressure and particle velocity were obtained during impact hammering for a total of eight piles. In addition, the construction contractor utilized a bubble curtain while hammering to reduce underwater noise levels generated by the pile driving. For two of the piles, acoustic measurements were taken with the bubble curtain in both active and inactive state to determine the effectiveness of that equipment in reducing pile driving noise levels.

This report presents the results of the aforementioned measurements. In the sections that follow the pile driving and bubble curtain equipment are discussed and the methods and apparatus used to obtain the acoustic measurements are described. The analyzed acoustic data are then presented, including examples of several pile driving waveforms and spectra, and the results are used to evaluate the effectiveness of the bubble curtain for reducing sound pressure and velocity levels from impact hammer pile driving.

2. Project description

This project will improve the efficiency of operations and the Eagle Harbor Maintenance Facility by converting an existing walk-on slip (Slip B) to a drive-on slip. The project involves demolition of existing structures and construction of new structures for the slip conversion. The project involves removal of existing structures and construction of new structures for slip conversion. Specifically the project includes the following:

- Removal of the two existing steel wing dolphins and one steel gangplank and it's single support pile.
- Installation of a new concrete trestle, a hydraulically actuated bridge support structure and bridge seat, two wing dolphins, one steel dolphin, and modifications to existing Pier 1 including site/slip utilities.

63 creosote-treated wood pilings will be removed from the area surrounding the Eagle Harbor Maintenance Facility to compensate for the habitat lost from adding up to 36 new pilings.

3. Experimental description

Acoustic pressure and particle velocity levels were measured while a total of eight cylindrical steel piles were installed next to a pier at the maintenance facility. The outside diameter of the piles was 30″ and the wall thickness was 1″. The length of the steel piles ranged from 75 ft. to 80 ft. and the weight of the piles per unit length was 311 lbs/foot. The piles were driven into the substrate using a Delmag 62 single-action diesel impact hammer suspended from a floating crane; a photograph of the impact hammer is shown in Figure 1(a). The weight of the hammer piston was 14,600 lbs. and the unit was capable of 36–50 blows per minute. The impact hammer featured four energy settings, labeled 1–4; energy setting 4 was used to hammer the first pile (T7) but all subsequent piles were hammered using energy setting 2.

The bubble curtain, which was used to mitigate underwater noise levels from the pile driving, was custom built by the construction contractor. Figure 1(b) shows a photograph of the active bubble curtain during the hammering of pile T7. The bubble curtain apparatus consisted of a 1″ thick cylindrical PVC sleeve, 44 ft. long and 47″ outside diameter, with two interior perforated aerating tubes. The diameter of the aerating tubes was 3″, the diameter of the air-hole perforations was 1/8″ and the hole spacing varied from 1.5″ to 4″. Figure 2(a) shows a photograph of the bubble curtain sheath during construction and Figure 2(b) shows a photograph of the aerating tubes inside the bubble curtain. One aerating tube was located at the base of the sleeve and the other was 10 ft. above the base. The bubble curtain sleeve was lowered over each pile before hammering and four heavy ballast chains at the base of the sleeve, with a combined weight of 2000 lbs., anchored the bubble curtain in place. While the bubble curtain was active, an air compressor supplied the aerating tubes at a rate of 300-350 CFM (cubic feet per minute) via four air hoses. The maximum capacity of the air compressor was 1600 CFM.

In order to measure underwater sound pressure and particle velocity levels during the pile driving, an acoustic sensor (described in detail in Section 4.2) was lowered off the side of an adjacent pier. The water depth at the pile driving location was 10 meters and the acoustic sensor was deployed mid water column at a depth of 5 meters. A plan view diagram of the pile layout, showing the approximate deployment locations of the acoustic sensor, is presented in Figure 3. The ten piles at the construction site were given the unique designations T1 through T10 in the engineering plan; in this report, specific piles are referred to by their designated names. Prior to each acoustic recording, the range from the acoustic sensor to each pile was measured using a Bushnell laser range finder. Table 1 lists the time, pile, range and deployment location for each acoustic recording.

(a) (b)

Figure 1: (a) Photograph of impact hammer and bubble curtain suspended from a floating crane. (b) Photograph of active bubble curtain during hammering of pile T7.

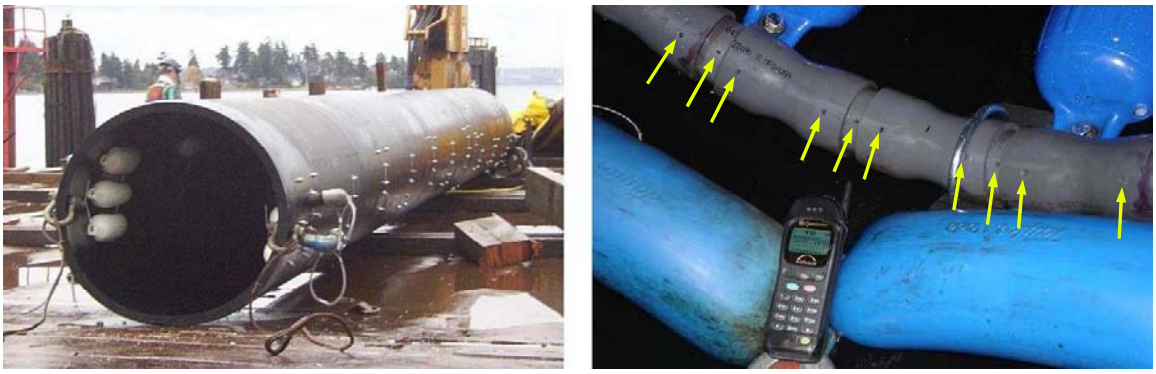

(a) (b)

Figure 2: (a) Photograph of bubble curtain sheath during construction. (b) Photograph of one of the 3″diameter aerating tubes affixed to the inside of the bubble curtain — yellow arrows indicate the positions of the 1/8″ diameter air holes.

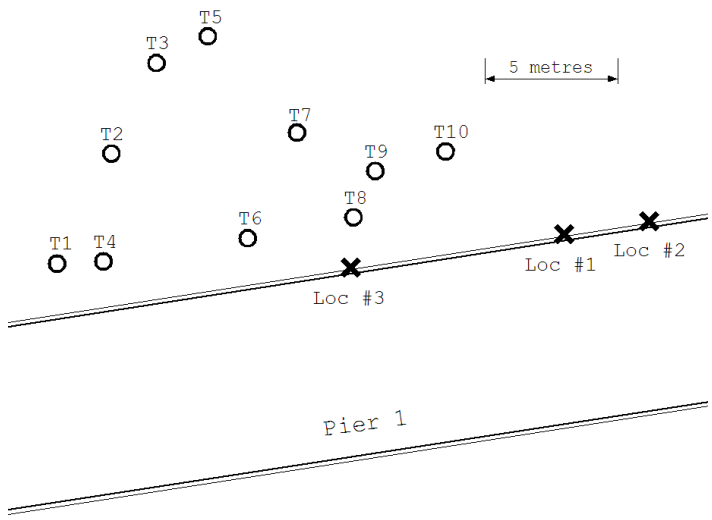

Figure 3: Plan view diagram of construction site showing the layout of the steel piles (labelled T1 through T10) and approximate deployment locations of the acoustic sensor (Loc #1, Loc #2 and Loc #3).

Table 1: Time of day, pile designation, measurement range and deployment location for each acoustic recording on 31 October 2005.

Rec #	Time	Pile	Range (m)	Position	Rec Type
1	12:07:04	T7	10	Loc #1	pressure only
2	12:32:17	T9	10	Loc #2	pressure only
3	12:55:14	T8	10	Loc #2	pressure and velocity
4	13:08:00	T6	15	Loc #2	pressure and velocity
5	13:19:19	T4	19	Loc #2	pressure and velocity
6	13:41:53	T5	16	Loc #2	pressure and velocity
7	14:54:58	T1	10	Loc #3	pressure and velocity
8	15:06:11	T2	9	Loc #3	pressure and velocity

4. Methodology

4.1. Theory

Acoustic particle velocity can be measured using the pressure gradient method, as described for example by Fahy (1977). It can be demonstrated mathematically, using Euler's linearized momentum equation, that the acoustic particle velocity may be computed from the time integral of the acoustic pressure gradient:

$$\mathbf{v} = -\int \frac{1}{\rho_o} \nabla p \, dt \qquad \text{(Eq. 1)}$$

where **v** is the vector particle velocity, ρ_0 is the fluid density and p is the acoustic pressure. Experimentally, the pressure gradient may be measured from the differential pressure between two closely spaced hydrophones:

$$\frac{\partial p}{\partial x} = -\rho_0 \frac{\partial v_x}{\partial t} \cong \frac{p(x+h/2) - p(x-h/2)}{h} \qquad \text{(Eq. 2)}$$

where p is acoustic pressure, v_x is the component of velocity along a single axis and h is the hydrophone spacing, which is small compared to the acoustic wavelength. The finite difference approximation of Equation 2 depends on small hydrophone separations relative to the acoustic wavelength and consequently there is an upper frequency limit for its practical application. It may be demonstrated that the amplitude error, in decibels, due to this finite-difference approximation is less than the quantity:

$$\varepsilon = 20\log_{10}\left(\frac{k_x h}{2\sin(k_x h/2)}\right) \qquad \text{(Eq. 3)}$$

where $k_x = 2\pi f/c$ is the acoustic wavenumber, f is the frequency of sound and c is the speed of sound in water.

4.2. Measurement apparatus

For the current study, the acoustic pressure gradient was measured using a custom built, multi-component hydroacoustic sensor designed by JASCO Research Ltd. The pressure gradient sensor was composed of a pyramidal frame supporting four Reson TC4043 hydrophones and a JASCO AIM attitude/depth sensor. The TC4043 hydrophones all had current NIST traceable calibrations; their nominal sensitivity was –201 dB re V/μPa. The four hydrophones were separated by 50 cm along three orthogonal axes (denoted as x, y and z) to measure the acoustic pressure gradient along each direction; the AIM sensor was oriented along the x-axis to monitor the orientation of the sensor. A schematic diagram and photograph of the pressure gradient measurement system are presented in Figure 4.

Pressure signals from the four hydrophones were fed via a shielded subsea cable to a notebook PC based acquisition system and sampled at 25 kHz per channel with 16-bit resolution. Subsequent software processing was used to compute differential pressure from the raw pressure waveforms. Depth, pitch and heading data from the AIM were fed via a separate cable to a Palm PDA and logged using custom software. Initial reference measurements of acoustic pressure were taken using a single Reson TC4034 hydrophone (nominal sensitivity –218 dB re V/μPa) connected via shielded hydrophone cables to an Ithaco 451M programmable gain amplifier. Pressure waveforms from the single TC4034 hydrophone were recorded to the notebook PC based acquisition system at 100 kHz sample rate.

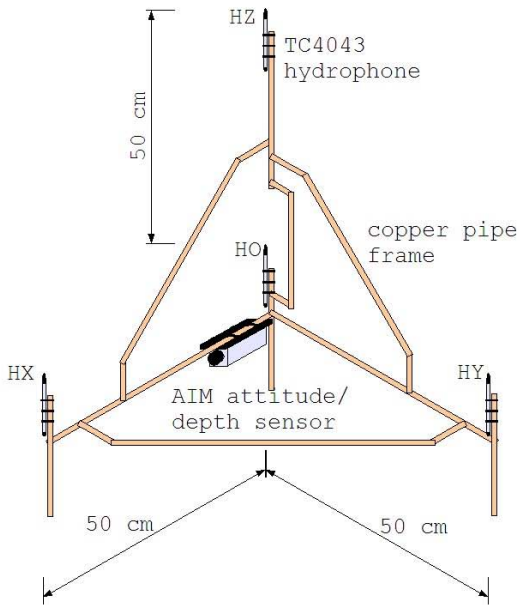

(a) **(b)**

Figure 4: (a) Schematic diagram of the pressure gradient sensor shown in isometric projection. Four Reson TC4043 hydrophones are located at the positions indicated HO (origin) HX (x-axis) HY (y-axis) and HZ (z-axis). The AIM attitude/depth sensor is oriented in the X-direction. The axial hydrophones HX, HY and HZ are all located 50 cm from the origin hydrophone HO. (b) Photograph of the pressure gradient sensor with attached hydrophone cables.

Sensitivity differences between the hydrophones were precisely characterized post field deployment via a cross-calibration procedure carried out as follows: the five hydrophones (four TC4043 and one TC4034) were taped together and simultaneously exposed to a swept reference signal (from 100 Hz to 2 kHz) from an underwater loudspeaker. The output signals from the hydrophones were simultaneously recorded and the frequency dependent sensitivity of the hydrophones was computed from the Fourier transforms of the calibration signals. The cross-calibration Fourier transforms were used to apply frequency dependent sensitivity corrections to the recorded pressure waveform data.

4.3. Data processing

Custom software, written in the IDL data analysis language, was used to compute acoustic particle velocity traces from the raw pressure waveforms. The processing steps were as follows:

1. The hydrophone preamplifiers' DC offset was removed from the pressure waveforms and a frequency dependent sensitivity correction, based on the cross-calibration, was applied to the data (see Figure 5).
2. The pressure traces were low-pass filtered at 1330 Hz to limit errors in the differential pressure calculation caused by aliasing of higher frequencies; 1330 Hz

corresponds to the 3 dB error point in the finite difference approximation, as given by Equation 3.

3. The signals at the three axial hydrophones, HX, HY and HZ, were subtracted from the origin hydrophone, HO, to yield the acoustic pressure gradient trace, $\nabla p(t)$. The pressure gradient trace was converted to vector particle acceleration, $\partial \mathbf{v}/\partial t$, by dividing by the water density, ρ_0, and the hydrophone spacing, h (see Equation 2).
4. The acceleration trace was high-pass filtered at 15 Hz to remove cumulative integration errors introduced by low-frequency noise in the acceleration data. High-pass filtering is required because the integral operator effectively multiplies the spectrum of the acceleration trace by the inverse of frequency, preferentially amplifying low frequency noise.
5. The acceleration trace was integrated over time to yield the three-component velocity trace, $\mathbf{v}(t)$. The velocity trace was de-trended and high-pass filtered at 5 Hz to remove small cumulative errors in the numerical integration.

4.4. Acoustic metrics

4.4.1. Sound pressure levels

For the current study the following metrics have been used for reporting received sound pressure levels from impulsive pile-driving noise:

1. **Peak Sound Pressure Level**, measured in dB re μPa:
   $$\pm L_{Pk} = 20\log_{10}\left(\max(\pm p(t))\right)$$
   Both peak overpressure ($+L_{pk}$) and peak underpressure ($-L_{pk}$) are provided.
2. **90% RMS Sound Pressure Level**, measured in dB re μPa. This metric is defined as the root-mean-square sound pressure level over a period that contains 90% of the pulse energy:
   $$L_{P90} = 20\log_{10}\left(\sqrt{\frac{1}{T_{90}}\int_{T_{90}} p(t)^2\,dt}\right)$$
3. **Sound Exposure Level**, measured in dB re μPa^2·s. For a single pulse, the sound exposure is defined as the integral of the squared sound pressure over the duration of the pulse event (see section 3.54 of ANSI S1.1-1994):
   $$L_E = 10\log_{10}\left(\int_T p(t)^2\,dt\right)$$
   For multiple impulsive events, the total sound exposure level is computed as the decibel sum of the sound exposure of the individual events.
   $$L_E^{(tot)} = 10\log_{10}\sum 10^{L_E^i/10}$$

In addition, pressure spectral levels are reported in units of dB re μPa/√Hz. Note that no frequency weighting (*e.g.*, A-weighting or C-weighting) has been applied to the acoustic measurements presented in this report.

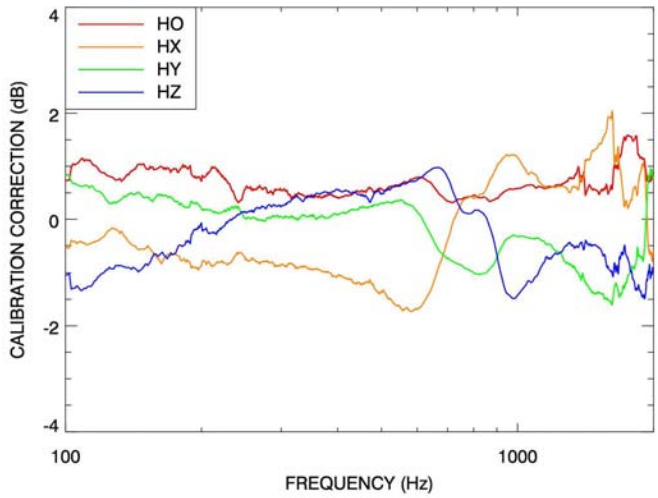

Figure 5: Plot of relative hydrophone sensitivity, versus frequency, as determined by cross-calibration procedure. Nominal hydrophone sensitivity is –201 dB re V/µPa.

4.4.2. Particle velocity levels

Vector-valued acoustic particle velocity traces (*x*, *y* and *z*) were numerically computed from differential pressure measurements, as described in Section 4.3. For each pulse, a velocity amplitude trace was constructed from the vector magnitude of the three axial traces:

$$v(t) = |\mathbf{v}(t)| = \sqrt{v_x(t)^2 + v_y(t)^2 + v_z(t)^2}$$

From the particle velocity amplitude trace, two velocity level metrics were computed:

1. **Peak Velocity Level**, the maximum dB level of the velocity amplitude trace:
$$L_{VPk} = 20\log_{10}(v_{\text{Peak}})$$
2. **90% RMS Velocity Level**, the root-mean-square dB level of the velocity amplitude trace over a time window containing 90% of the integrated square velocity:
$$L_{V90} = 20\log_{10}\left(\sqrt{\int_{T90} v(t)^2\,dt}\right)$$

Note that the reference for particle velocity levels is nm/s, as defined in ANSI standard S1.1-1994. In addition, particle velocity spectral levels are reported in units of dB re nm/s/√Hz.

5. Measurement results

During the pile driving construction activities at Eagle Harbor maintenance facility on 31 October 2005, underwater sound pressure measurements were obtained for a total of eight piles and acoustic particle velocity measurements were obtained for a total of six piles. All piling measurements were taken off the side of a pier (as shown in Figure 3), at

a depth of 5 meters in 10 meter deep water, close to several docked vessels and floating construction barges.

The raw pressure waveform data were processed according to the procedures described in Section 4.3 to obtain decibel sound pressure level and particle velocity level metrics. Average values for the sound pressure and particle velocity metrics for each pile are given in Table 2 and Table 3. Note that at the start of hammering for each pile there were one or two blows where the impact hammer piston did not deliver a full stroke to the pile; these weak initial blows were discarded from the average metrics presented in the tables. For piles T7 and T8, separate metrics are provided in Table 2 for pressure measurements with the bubble curtain active and inactive. These data show that, on average, the active bubble curtain reduced peak pressure levels by 9.1 dB (combined overpressure and underpressure) and RMS pressure levels by 8.6 dB. Similarly, the velocity data for pile T8 in Table 3 show that, on average, the active bubble curtain reduced peak velocity levels by 11.4 dB and RMS velocity levels by 12.1 dB. In addition, the active bubble curtain consistently increased the pulse length, T_{90}, of both the pressure and velocity traces. The peak pressure rise time could not be computed because the bubble curtain altered the shape of the pile driving pulse so that the maximum pressure was observed many oscillations after the initial onset (*c.f.*, Figure 6). This made the calculation of the initial rise-time problematic at best, since it was not possible to identify an unambiguous peak in the pile driving data.

Twenty pressure traces from the hammering of pile T8 are presented in Figure 6 showing the comparison between the active and inactive bubble curtain. Multiple peaks in the pressure waveforms in Figure 6 were caused by multipath reflections from the water surface and seabed and from the hulls of nearby vessels and barges. A comparison of average pressure spectral levels for pile T8 with the bubble curtain active and inactive is presented in Figure 7. These spectra show that, although the bubble curtain attenuated the pile hammering noise at most frequencies, the attenuation was not uniform. Indeed at certain frequencies, (*e.g.*, at 245 Hz and 1230 Hz) the bubble curtain appears to have enhanced, rather than attenuated, the hammering noise. Note that these enhanced peaks were a repeatable feature for all strikes on pile T8, since the spectra presented in Figure 7 are mean spectral levels over all hammer blows; however, the contribution of these narrow peaks to the overall received level is very small. Absorption and scattering of sound by a bubble curtain is a complex physical process and it is beyond the scope of the current study to identify the precise physical mechanism that causes these resonances.

Triaxial velocity traces for pile T8, for the same twenty hammer blows, are presented in Figure 8. This figure shows that maximum peak levels from pile T8 were observed on the X-channel (radial) velocity trace. This observation is consistent with the logged orientation of the pressure gradient sensor during the measurement: the digital compass indicated that the X-axis of the instrument was pointed in the direction of pile T8 to within 10 degrees. In addition, when the bubble curtain was inactive, the Z-channel (vertical) velocity trace consistently exhibited a strong negative deviation at the onset of the pile hammering pulse. This downward particle motion is likely attributable to the downward movement of the pile upon impact of the pile driving hammer. Figure 9 shows average velocity spectral levels for pile T8 for the three measurement axes, with the bubble curtain active and inactive. As with pressure, the bubble curtain's attenuation

of the velocity spectra was not uniform with frequency. In addition, comparing Figure 9 with Figure 7 one can see that lower frequencies in the velocity spectral levels are clearly enhanced relative to the pressure spectral levels. This amplification of lower frequencies in the velocity trace is due to the integration process linking velocity and differential pressure in Equation 1: the integral operator effectively divides the differential pressure spectrum by frequency, *f*, thus attenuating high frequencies in the velocity trace relative to low frequencies. This is a real physical consequence of the relationship between differential pressure (or, equivalently, acceleration) and velocity and is not an artefact of the data processing technique.

Table 2: Mean sound pressure levels and total sound exposure levels measured during hammering of each individual pile. The five metrics provided in the table are mean peak overpressure (+Peak), mean peak underpressure (–Peak), mean 90% RMS level (RMS90), total sound exposure level (SEL) and mean 90% pulse period (T_{90}). Separate levels are given for recording periods where bubble curtain was active (on) and inactive (off).

				Sound Level (dB re μPa†)				
Pile	**Range (m)**	**Bubbler**	**Strikes**	**+Peak**	**–Peak**	**RMS90**	**SEL**	**T_{90} (msec)**
T5	16	‡OFF	25	203.7	202.2	192.5	193.0	40.4
T7	10	OFF	9	202.1	203.5	192.2	188.7	45.5
T8	10	OFF	15	202.8	204.2	192.6	190.6	38.1
T1	10	ON	13	193.5	196.6	182.6	183.1	84.1
T2	9	ON	8	195.7	196.6	185.5	182.1	53.2
T4	19	ON	15	192.5	190.4	181.4	180.9	52.8
T6	15	ON	18	195.5	192.7	185.0	184.0	39.0
T7	10	ON	11	194.3	194.1	184.2	182.0	49.9
T8	10	ON	12	193.2	194.4	183.3	181.9	55.6
T9	10	ON	9	191.1	189.7	180.3	177.1	49.3

† Units of sound pressure (L_{Pk}, L_{P90}) are dB re μPa and units of sound exposure (L_E) are dB re μPa^2·s.
‡ The bubble curtain sheath was altogether absent during hammering of pile T5.

Table 3: Mean velocity levels measured during hammering of each individual pile. The three metrics provided are mean peak velocity (Peak), mean 90% RMS velocity (RMS90) and mean 90% pulse period (T_{90}). Separate levels are given for recordings where bubble curtain was active (on) and inactive (off).

				Velocity Level (dB re nm/s)		
Pile	**Range (m)**	**Bubbler**	**Strikes**	**Peak**	**RMS90**	**T_{90} (msec)**
T5	16	†OFF	25	137.9	128.3	58.1
T8	10	OFF	15	140.5	129.4	61.7
T1	10	ON	13	130.5	117.6	223.9
T2	9	ON	8	132.7	119.2	185.3
T4	19	ON	15	129.1	114.6	198.5
T6	15	ON	18	130.7	119.0	82.2
T8	10	ON	12	129.1	117.3	141.9

† The bubble curtain sheath was altogether absent during hammering of pile T5.

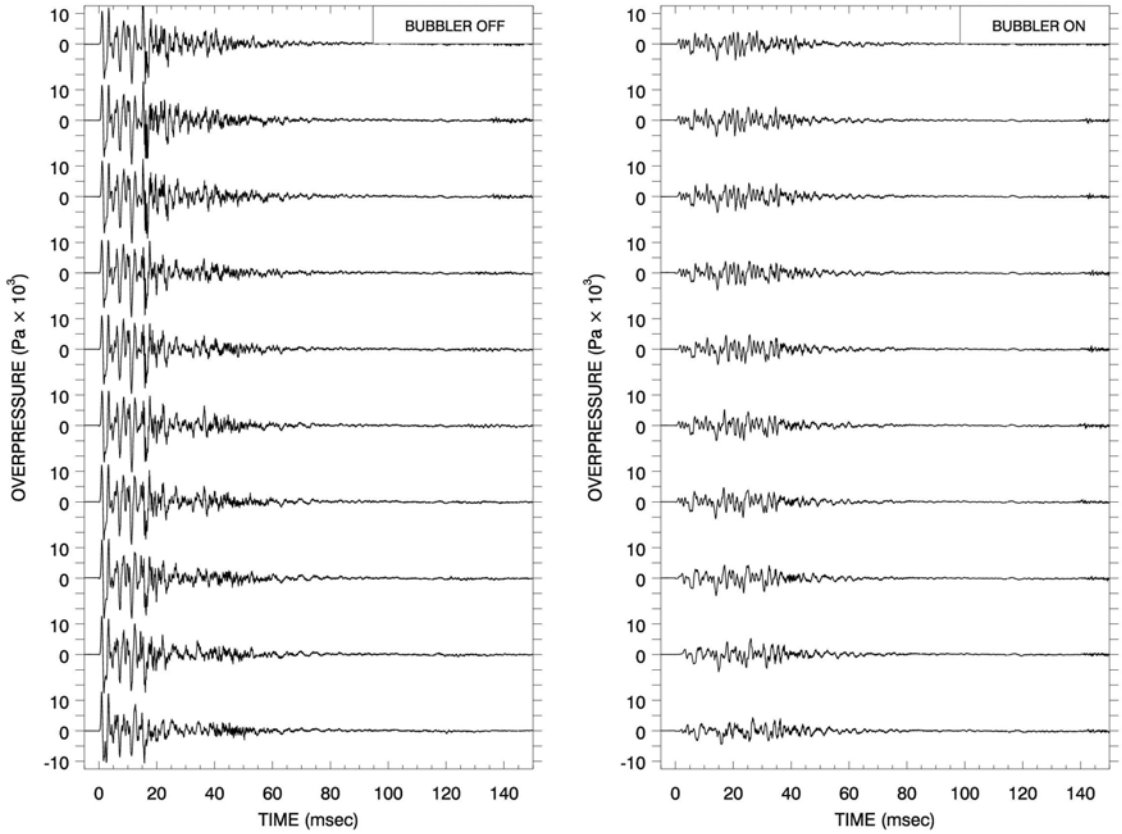

Figure 6: Pressure waveforms from impact hammering of pile T8 showing comparison between inactive bubble curtain (left) and active bubble curtain (right). Measurements were taken at 10 meters horizontal range and 5 meters depth.

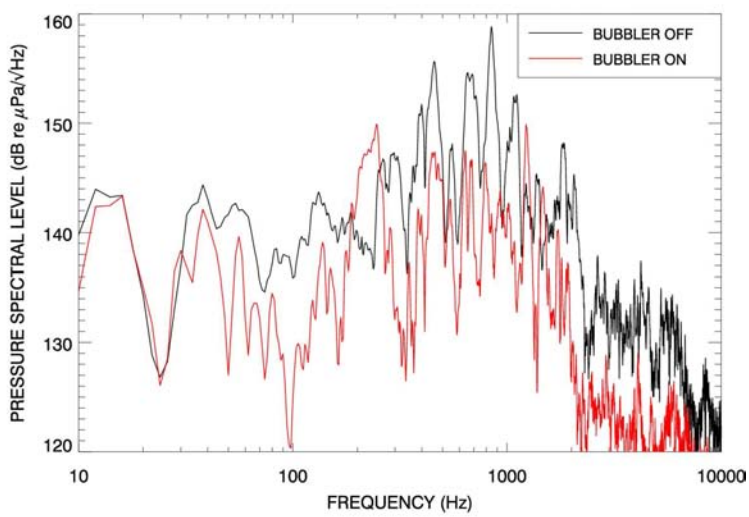

Figure 7: Average pressure spectral levels for pile T8 impact hammering waveforms. The inactive bubble curtain spectrum is shown in black and the active bubble curtain spectrum is shown in red.

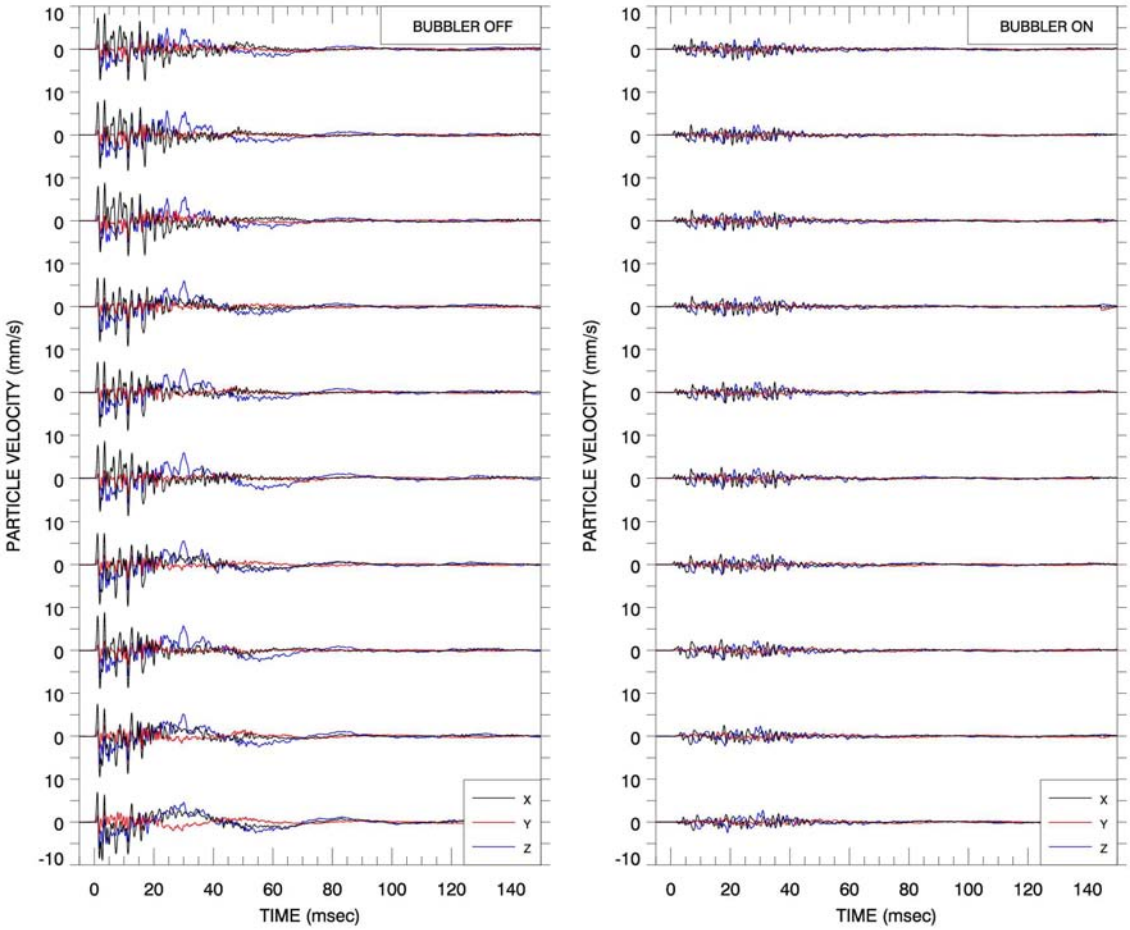

Figure 8: Triaxial particle velocity traces from hammering of pile T8 showing comparison between inactive bubble curtain (left) and active bubble curtain (right). Measurements were taken at 10 meters horizontal range and 5 meters depth.

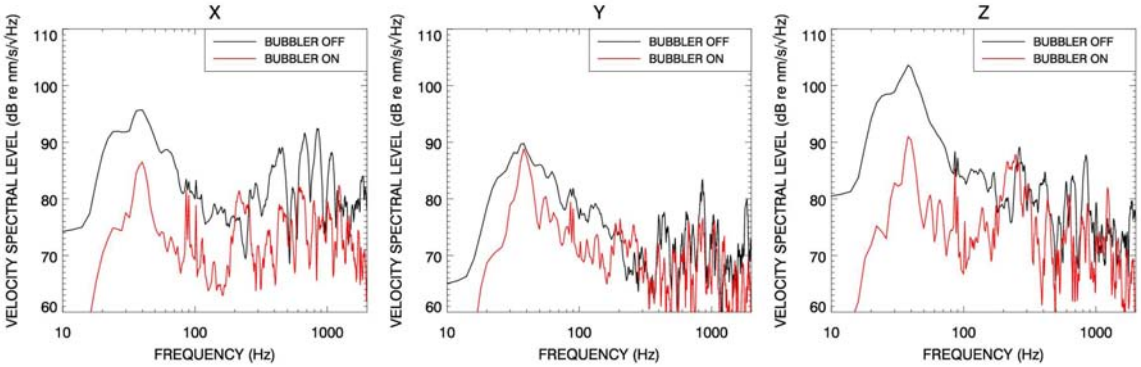

Figure 9: Average X, Y and Z velocity spectral levels for pile T8 impact hammering traces. The inactive bubble curtain spectra are shown in black and the active bubble curtain spectra are shown in red.

6. Summary

Acoustic sound pressure and particle velocity measurements were obtained from impact hammer pile driving of eight 30 in. diameter steel piles at the Eagle Harbor maintenance facility on 31 October 2005. Sound pressure and particle velocity waveforms were measured at 5 meters depth, in 10 meters of water, at horizontal ranges from 9 to 19 meters. Underwater noise levels from the pile driving were mitigated using a 47 in. diameter bubble curtain sleeve around the piles, with an airflow rate of approximately 350 CFM; the effectiveness of the bubble curtain was evaluated by comparing pile driving sound levels with the bubble curtain activated and deactivated. With the bubble curtain deactivated the highest sound levels were measured from pile T8 at 10 meters range: 204.2 dB re μPa peak pressure and 190.6 dB re μPa RMS pressure, 140.5 dB re nm/s peak velocity and 132.7 dB re nm/s RMS velocity. With the bubble curtain activated the highest sound levels were measured from pile T2 at 9 meters range: 196.6 dB re μPa peak pressure and 185.5 dB re μPa RMS pressure, 132.7 dB re nm/s peak velocity and 119.2 dB re nm/s RMS velocity. Measurements from pile T7 and T8 at 10 meters range indicated that, on average, the active bubble curtain attenuated peak pile driving sound pressure levels by 9.1 dB and peak particle velocity levels by 11.4 dB. Thus the bubble curtain proved effective in mitigating both sound pressure and particle velocity levels generated by the pile driving.

7. Literature cited

ANSI S1.1 (1994) *American National Standard Acoustical Terminology*.

Fahy, F.J. (1977). "Measurement of acoustic intensity using the cross-spectral density of two microphone signals." J. Acoust. Soc. Am. **62**(4), pp. 1057–1059.